JPE 18-4-9

https://doi.org/10.6113/JPE.2018.18.4.1037
ISSN(Print): 1598-2092 / ISSN(Online): 2093-4718

Reconfigurable Selective Harmonic Elimination Technique for Wide Range Operations in Asymmetric Cascaded Multilevel Inverter

Kavitha R* and Rani Thottungal†

†,*Dept. of Electrical and Electronics Engineering, Kumaraguru College of Technology, Coimbatore, India

Abstract

This paper presents a novel reconfigurable selective harmonic elimination technique to control harmonics over a wide range of Modulation Indexes (MI) in Multi-Level Inverter (MLI). In the proposed method, the region of the MI is divided into various sectors and expressions are formulated with different switching patterns for each of the sectors. A memetic BBO-MAS (Biogeography Based Optimization - Mesh Adaptive direct Search) optimization algorithm is proposed for solving the Selective Harmonic Elimination - Pulse Width Modulation (SHE-PWM) technique. An experimental prototype is developed using a Field Programmable Gate Array (FPGA) and their FFT spectrums are analyzed over a wide range of MI using a fluke power logger. Simulation and experimental results have validated the performance of the proposed optimization algorithms and the reconfigurable SHE-PWM technique. Further, the sensitivity of the harmonics has been analyzed considering non-integer variations in the magnitude of the input DC sources.

Key words: Modulation index, Multilevel inverter, SHE-PWM technique, THD

I. INTRODUCTION

Multi-Level Inverters (MLIs) have emerged as a prospective inverter technology in AC motor drives and distributed energy generation systems due to its advantages in terms of reduced switching losses, improved harmonic profile, improved Electro-Magnetic Compatibility (EMC) and reduced voltage stress across the devices. Various MLI topologies exist in the literature and the Cascaded H-bridge Multi-Level Inverter (CMLI) is the most popular topology owing to its modular structure. The challenges that attract most attention in CMLI are providing cost effective topologies with reduced switch count, further enhancements of the harmonic profile and reduction of the switching losses [1], [2]. The Asymmetric Cascaded Multilevel Inverter (ACMLI) was proposed to increase the number of levels with a reduced switch count [3]. Selective Harmonic Elimination Pulse Width Modulation (SHE-PWM) and Minimization of Total Harmonic Distortion (MTHD) are the promising low frequency switching strategies that reduce the switching losses in CMLI [4]-[6].

The objective function of SHE-PWM is non-transcendental in nature and difficult to solve in high dimensional space. In addition, the spectral performances offered by the SHE-PWM technique differ with respect to variation in the MI.

The multilevel inverters in adjustable-speed motor drives have to dynamically control the speed of motors ranging from very low speeds to the rated speed. These drives demand the effective voltage control of MLIs in a wide range of MI [7]. In a Dynamic Voltage Restorer (DVR), when the depth of voltage sag is shallow, the inverter stage of the DVR needs to operate with a very low MI while generating a high quality compensated output waveform [8]. Multilevel inverters form the mainstay of the above products. Thus, they have to be sized to operate proficiently over a wide range of MI.

The traditional SHE-PWM modulation technique does not provide a feasible solution for the complete range of MI. Thus, it is said to work in a narrow operating range. This paper presents a hybrid algorithm for solving the SHE-PWM technique in a high dimensional space and a reconfigurable SHE-PWM technique to operate over a wide operating range of MI. Several optimization techniques such as the analytical

Manuscript received Jul. 20, 2017; accepted Feb. 27, 2018
Recommended for publication by Associate Editor Yun Zhang.
†Corresponding Author: kavithain2@yahoo.com
Tel: +91-9843460448, Kumaraguru College of Technology
*Dept of Electr. & Electron. Eng, Kumaraguru College of Tech., India

methods [9], [10], global search meta-heuristic techniques [11]-[15] and hybrid techniques [16], [17] have been employed in the literature to solve the SHE-PWM technique. In [16], a hybrid PSO-NR (Particle Swarm Optimization – Newton Raphson) algorithm was proposed to eliminate the low-order harmonics in modular MLI. In [17], the Adaptive Neuro-Fuzzy Inference System - Artificial Bee Colony (ANFIS-ABC) algorithm eliminates low order harmonics in MLI. However, the feasible solution range exists only in the range of MI from 0.5 to 1.

The harmonic minimization technique presented in [18] provides a feasible solution only in the range of MI from 0.83 to 1. The authors of [19] focused on acquiring the wide range operation of MI by applying Modified Selective Harmonic Elimination Pulse Width Modulation (MSHE-PWM). However the maximum switching frequency is increased to 450Hz. Hybrid Modified Cuckoo Search Algorithm Self- Adaptive Mutation (MCSA-SAM) has been presented in [20] with MTHD as the objective function. It also considers the effect of a snubber and blanking time in a nine level inverter. The objective function remains the same and does not resolve the problem of the narrow operating range of MI. An improved colonial competitive algorithm was proposed in [21] for various operating points, while considering asymmetrical fixed DC-link voltages. Selective Harmonic Elimination - Pulse Amplitude Modulation (SHE-PAM) was introduced in [22], where dc sources are utilized as an extra degree of freedom in addition to switching angles. However, dc chopper circuits with precise voltage control are required for varying the voltage levels. A modified fundamental SHE-PWM technique was devised in [23]-[25] by relaxing the constraint associated with the number of harmonics to be eliminated. The Transistor-Clamped H-Bridge (TCHB) inverter based CMLI topology was employed in [26] with SHE-PWM technique. However, the analysis was only carried out with the MI as 1.

The main contributions of this paper are as follows. A potential algorithmic exemplar memetic algorithm, a hybrid combination of local and global search algorithms, is developed in order to improve the speed of convergence and to obtain optimal global solutions. A reconfigurable SHE-PWM technique is proposed to eliminate all of the intended harmonics over a wide range of Modulation Indexes (MI). Further, a sensitivity analysis of harmonics is carried out with the non-integer magnitude of input DC sources. Experimental results and a FFT spectrum are presented to validate the performance of the reconfigurable SHE-PWM technique.

II. General Structure of the ACMLI Topology

In a Symmetric Cascaded H-bridge Multilevel Inverter (SCMLI) the ratio of the input DC source remains equal. SCMLI generates a seven level output voltage with three

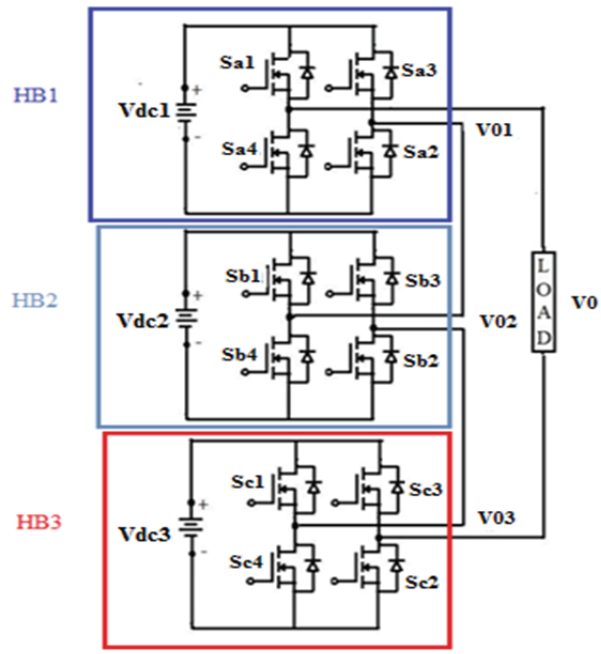

Fig. 1. Structure of the ACMLI topology.

H-bridge cells. To achieve the elimination of a larger number of harmonics and to enhance the power quality, the number of voltage levels in the output needs to be increased.

An attempt to increase the number of levels in the traditional SCMLI leads to a large number of H-bridge cells. The ACMLI topology in Fig. 1 is developed with a different ratio of the input DC source in order to increase the number of levels and to reduce the switch count.

The design considerations for ACMLI are as follows:

1) The series-connected H-bridge cells require distinct dc sources that are arranged in increasing order, so that the nth H-bridge cell presents the highest voltage step.

$$Vdc1 \le Vdc2 \le \ldots\ldots\ldots\ldots \le Vdcn\text{-}1 \le Vdcn.$$

2) The normalized ratio of the synthesized voltage step δ_n given by equation (1) should be a natural number (N) in order to generate equally spaced uniform levels of voltage waveforms. This in turn requires constant regulated dc sources.

$$\frac{Vdc3}{Vdc1} = \delta_n,\ \delta_n \in N \tag{1}$$

The switching function and output voltage of an inverter are related by equation (2) and the number of voltage levels (m) generated by n H-bridge cells is given by equation (3).

$$V_0 = \sum_{j=1}^{n} S_j * Vdc_j\,; \qquad S_j \in \{-1, 0, +1\} \tag{2}$$

$$m = 1 + 2\sum_{j=1}^{n} Vdc_j \tag{3}$$

The values of the input DC sources (Vdc1, Vdc2, and Vdc3) are provided in a ratio of 1:2:3 in the H bridges (HB1, HB2, HB3) to obtain a 13-level output voltage in ACMLI. The switches Sa1 and Sa2 are turned on to generate Vdc1, the

switches Sa3 and Sa4 are turned on to generate –Vdc1, and the switches Sa1 and Sa3 or Sa2 and Sa4 are turned on to bypass the voltage source Vdc1. Switching is performed in a similar fashion in HB2 and HB3 to obtain corresponding voltages. The prototype is constructed with low voltage input sources. Thus, a MOSFET is employed as a switching device in all of the H bridges.

III. Traditional SHE-PWM Technique

The output voltage equation for a thirteen-level ACMLI in the traditional SHE-PWM is expressed in [13] and indicated by equation (4) with the constraint $0 \leq \theta_i \leq \pi/2$.

$$V_{hn} = \frac{4V_{dc}}{n\pi}\left[\sum_{i=1}^{6} \cos n\theta_i\right] \quad (4)$$

The objective function of SHE-PWM for a 13-level ACMLI is given by equation (5). The Selective Harmonic (SH) % for a 13-level ACMLI is denoted by equation (6).

$$f_{SHE\text{-}PWM} = \min\left\{\left(100\frac{V_1^* - V_1}{V_1^*}\right)^4 + \sum_{n=5,7,11,13}^{17} \frac{1}{n}\left(50\frac{V_{hn}}{V_1}\right)^2\right\} \quad (5)$$

$$SH(\%) = \frac{V_{h5}+V_{h7}+V_{h11}+V_{h13}+V_{h17}}{V_{h1}} * 100 \quad (6)$$

IV. Memetic Algorithm

In the memetic BBO-MAS algorithm, initially a global search algorithm BBO, is applied to trace the region of the solution. Then a MAS algorithm is applied to obtain the global minimal fitness value with a rapid convergence. The BBO algorithm primarily deals with the migration of species from one island to another [27]. The geographic areas that are best suited for biological species to survive are said to have a high Habitat Suitability Index (HSI) and the parameter that indicates this region is referred to as the Suitability Index Variable (SIV). The movement of existing species from an island is emigration and the arrival of new species on an island is immigration. The advantages of BBO over other heuristic approaches are stated below. BBO maintains its solution set from one iteration to the next, even when their characteristics change. In Particle Swarm Optimization (PSO), solutions are highly dependent on the position and velocity coefficient. In BBO, solutions are updated directly through migration. The emigration rate and immigration rate determine the best region for the movement of species and the mutation rate for each set of solutions. The MAS algorithm performs searches in two stages, namely the search step and the poll step. In the search step, the algorithm searches a set of points referred to as a mesh around a current point. The mesh is created by adding up a current point to a scalar multiple of a set of vectors expressed as a pattern [28]. The memetic algorithm has been employed in economic dispatch problem [29], the design of antennas [30] and the optimal design of electro-magnetic systems [31].

TABLE I
Parameters Used in the BBO Algorithm

Parameters	Values
Number of habitat (H)	3
Probability of habitat modification (P_i)	1
Population size	50
Number of iterations	3
Elitism parameter	2
Probability of mutation (P_{max})	0.005
Step size (Δt), Maximum immigration rate (λ_s) and emigration rate (μ_s)	1

A. BBO Algorithm for Solving the Objective Function

1) Initialize the parameters of the BBO as listed in Table I. The switching angles are generated at random and are represented by SIV = [θ_1, θ_2, θ_3]. The boundary constraint for the SIV is $0<\theta_i<90^o$ since it obeys quarter wave symmetry.

$$H = SIV = [\theta_1, \theta_2, \theta_3]$$

2) The fitness value is calculated for the objective function $f_{SHE\text{-}PWM}$ and it is represented by the HSI. Based on the HSI, elite habitats are identified.
   a. Perform migration operation on the SIV of every non-elite habitat.
   b. Based on λ_i decide the probability of whether to immigrate to X_i. Choose the emigrating island X_i with a probability of P_i and replace it with a new X_i.
   c. A mutation operation is performed on the non-elite habitat. In the mutation operation, replace the selected habitat by a random habitat set.
   d. Proceed with step (a) for the next iteration and the looping continues for 150 iterations.
   e. Initialize the switching angle values obtained from BBO as the current point (X_{best}) for the MAS with the mesh size (Δ^m).
   f. Generate a set of vectors {M} by multiplying the pattern vector L_i by Δ^m; ($M=L_i * \Delta^m$).
   g. Add M to X_{best}; $X= X_{best}+ M$.
   h. Compute the objective function and compare whether the objective function value is less than the best fitness (F_{best}) obtained so far. If the condition is satisfied it is referred as a successful search.
   i. If the poll is successful, then $X_{best}=X$ and $F_{best}=F$, and the mesh size is expanded by multiplying Δ^m by 2.
   j. If the poll is unsuccessful, multiply Δ^m by 0.5.
   k. Proceed to step f.

SHE-PWM is an offline computation technique. Thus, the CPU running time is considered for analyzing the computation complexity. The CPU running times in PSO and BBO for 200 iterations are 83 Sec and 69 Sec, respectively. In the BBO-MAS algorithm convergence occurs within 160

TABLE II
COMPARISON OF THE BBO-MAS ALGORITHM WITH THE BBO AND PSO

Algorithm	θ_1^o	θ_2^o	θ_3^o	θ_4^o	θ_5^o	θ_6^o	$f_{SHE-PWM}$
PSO	5.73	16.05	26.52	38.11	53.15	60.89	0.2247
BBO	6.34	17.20	24.86	38.09	49.60	65.61	0.084
BBO-MAS	7.71	16.74	24.42	36.51	53.03	63.26	2.52E-06

Targeted Harmonics and THD

Algorithm	h5 (%)	h7 (%)	h11 (%)	h13 (%)	h17 (%)	SH (%)	THD Phase (%)
PSO	0.52	2.16	0.51	1.36	0.09	4.65	7.9
BBO	0.65	0.09	0.12	1.51	1.38	3.7	6.96
BBO-MAS	0.001	0	0.004	0.005	0.002	0.01	7.64

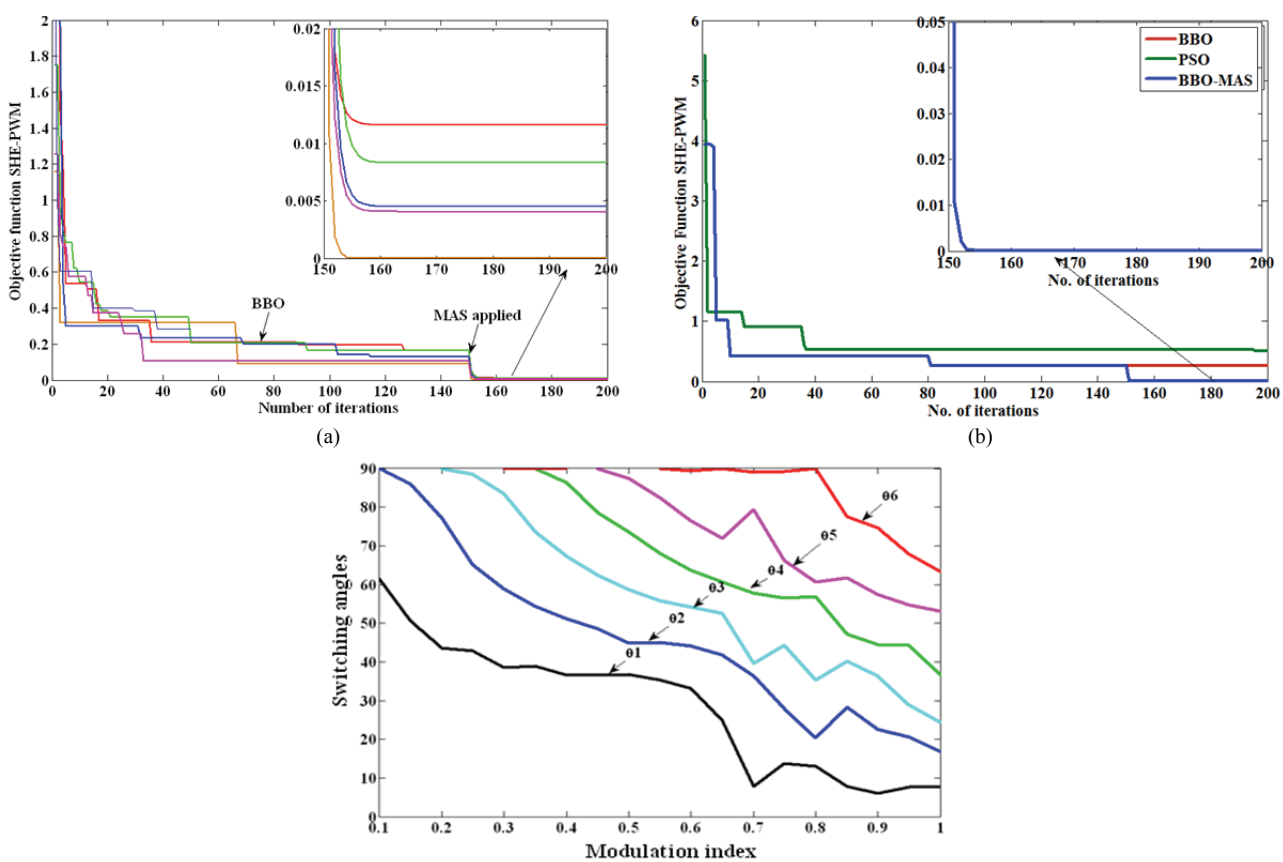

Fig. 2. Plots showing: (a) Convergence of the BBO-MAS algorithm; (b) Comparisons of the BBO-MAS algorithm with the BBO and PSO; (c) Switching angles obtained with the BBO algorithm.

iterations for all 6 runs as shown in Fig. 2(a) and the CPU running time is 76.22 sec.

The switching angles are calculated offline and then given as firing pulses using a FPGA for implementation in hardware. It is obvious from the Fig. 2(b) and Table II that for MI=1, the global minimal value of the objective function is obtained in the BBO-MAS algorithm when compared to the PSO and BBO algorithms. The BBO algorithm has given a residual of 3.7% of the specified harmonics in the output. In the BBO-MAS algorithm the specified harmonics are completely eliminated and are almost equal to 0.01%. The optimized switching angles obtained for the entire range of MI are shown in Fig. 2(c). It is observed that the switching angles converge to 90° and that the number of DOF to control the harmonics is reduced with variation in the MI. The convergence of the switching angles occurs at the point of

TABLE III
RANGE OF THE MODULATION INDEX AND THE SWITCHING ANGLE DISTRIBUTION

Sector	Equation for V_{hn}
1	$\frac{4Vdc}{n\pi}(\cos(n\theta_1)+\cos(n\theta_2)+\cos(n\theta_3)+\cos(n\theta_4)+\cos(n\theta_5)+\cos(n\theta_6))$
2	$\frac{4Vdc}{n\pi}(\cos(n\theta_1)+\cos(n\theta_2)+\cos(n\theta_3)+\cos(n\theta_4)+\cos(n\theta_5)-\cos(n\theta_6))$
3	$\frac{4Vdc}{n\pi}(\cos(n\theta_1)+\cos(n\theta_2)+\cos(n\theta_3)+\cos(n\theta_4)-\cos(n\theta_5)+\cos(n\theta_6))$
4	$\frac{4Vdc}{n\pi}(\cos(n\theta_1)+\cos(n\theta_2)-\cos(n\theta_3)+\cos(n\theta_4)+\cos(n\theta_5)-\cos(n\theta_6))$
5	$\frac{4Vdc}{n\pi}(\cos(n\theta_1)-\cos(n\theta_2)+\cos(n\theta_3)+\cos(n\theta_4)-\cos(n\theta_5)+\cos(n\theta_6))$
6	$\frac{4Vdc}{n\pi}(\cos(n\theta_1)-\cos(n\theta_2)+\cos(n\theta_3)-\cos(n\theta_4)+\cos(n\theta_5)-\cos(n\theta_6))$

MI=0.83 itself. Thus, the thirteen-level ACMLI can operate with a feasible solution only in the region of MI from 0.83 to 1.

V. RECONFIGURABLE SHE-PWM TECHNIQUE

In the proposed reconfigurable SHE-PWM technique, the objective is to keep the number of DOF (switching angles) as the same irrespective of variations in the MI. To maintain the DOF, the switching angles must satisfy the condition $0 \leq \theta_i \leq 90^0$ and multiple switching is performed at the same level by swapping the polarity of the waveform. The MI region is divided into sectors equal to the number of switching angles. The formulas for deciding the lower and upper ranges for dividing the sector are given by equations (7) and (8).

$$\text{Lower bound } n(m)=\frac{m-1}{N}+0.01 \quad (7)$$

$$\text{Upper bound } n(m)=\frac{m}{N} \quad (8)$$

Where N is the number of switching angles and m= N, N-1,..1. Thirteen-level ACMLI has six switching angles. Thus, the region of the MI is classified into 6 different sectors.

The voltage harmonic is represented by equation (9) for a thirteen-level ACMLI and the polarity of the cosine terms is decided based on the sector in which the MI is located.

$$V_{hn}=\frac{4V_{dc}}{n\pi}[\cos n\theta_1 \pm \cos n\theta_2 \pm \cos n\theta_3 \pm \cos n\theta_4 \pm \cos n\theta_5 \pm \cos n\theta_6] \quad (9)$$

With 6 switching angles a total of 2^6 (64) different sets of expressions and switching patterns are possible. The switching patterns have to satisfy predefined conditions. Only the rising edge should occur in the beginning and two adjacent falling edges cannot occur simultaneously. The sector and switching pattern expressions are indicated in Table III and upper and lower bounds are specified by Table IV. The waveforms corresponding to various sectors are shown in Fig. 3. In the traditional SHE-PWM technique in sector 2 at MI=0.75, a single switching angle converges to 90° and generates an eleven-level output with DOF as 5. The reconfigurable SHE-PWM technique provides an eleven-level output voltage and still maintains the DOF at 6 by switching twice in the upper level. Similarly, in all of the ranges of MI the DOF is maintained at six to achieve a reduction of all the intended harmonics.

TABLE IV
MATHEMATICAL SEGMENTATION OF MI

Sector	m	Lower Bound	Upper Bound	Level
1	6	0.84	1	13
2	5	0.68	0.83	11
3	4	0.51	0.67	9
4	3	0.34	0.50	7
5	2	0.18	0.33	5
6	1	0	0.17	3

A. Power Distribution Analysis

The output voltage waveform of an individual H-bridge cell is indicated in Fig. 4. The expression for a switching pattern with MI=1 is represented by a Fourier series as shown in equations (10-12).

$$So_1 = \frac{4}{\pi}\left(\cos n\theta_1 - \cos n\theta_2 + \cos n\theta_4 - \cos n\theta_5 + \cos n\theta_6\right) \quad (10)$$

$$So_2 = \frac{4}{\pi}\left(\cos n\theta_2 - \cos n\theta_3 + \cos n\theta_5\right) \quad (11)$$

$$So_3 = \frac{4}{\pi}(\cos n\theta_3) \quad (12)$$

Thus, the output voltage and current are represented by equations (13-14)

$$Vo = Vdc1So_1 + Vdc2So_2 + Vdc3So_3 \quad (13)$$

Assuming $Vdc1=K_1Vdc$; $Vdc2=K_2Vdc$; $Vdc3=K_3Vdc$.

$$\text{Vo} = \text{Vdc}(K_1So_1 + K_2So_2 + K_3So_3) \text{ ; Io=Vo/R} \quad (14)$$

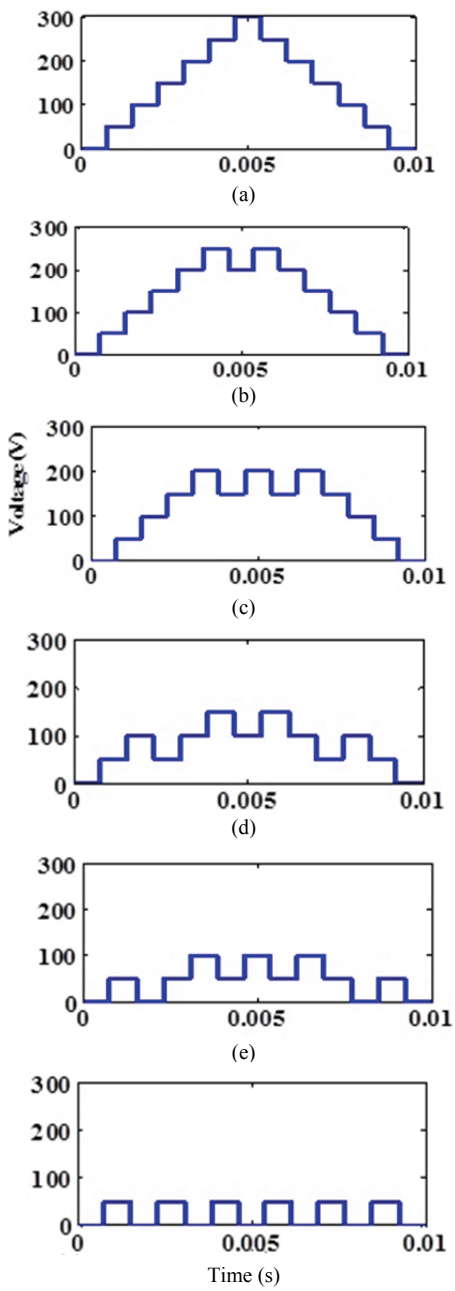

Fig. 3. Positive half cycle of a 13 level inverter under different modulation indexes: (a) MI = 0.84 to 1; (b) MI = 0.68 to 0.83; (c) MI = 0.51 to 0.67; (d) MI = 0.34 to 0.50; (e) MI = 0.18 to 0.33; (f) MI = 0 to 0.17.

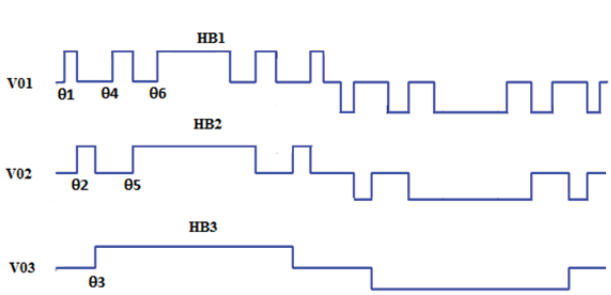

Fig. 4. Voltage waveform of an individual H-bridge cell.

TABLE V
OPTIMIZED SWITCHING ANGLES IN THE RECONFIGURABLE SHE-PWM

MI	θ_1^o	θ_2^o	θ_3^o	θ_4^o	θ_5^o	θ_6^o
1.00	7.71	16.74	24.42	36.51	53.04	63.26
0.75	7.46	22.50	23.22	53.04	71.89	78.17
0.65	7.29	24.76	41.87	59.72	65.57	70.77
0.45	17.59	24.31	41.84	48.38	62.50	82.77
0.25	22.11	24.58	38.20	61.43	67.77	73.85

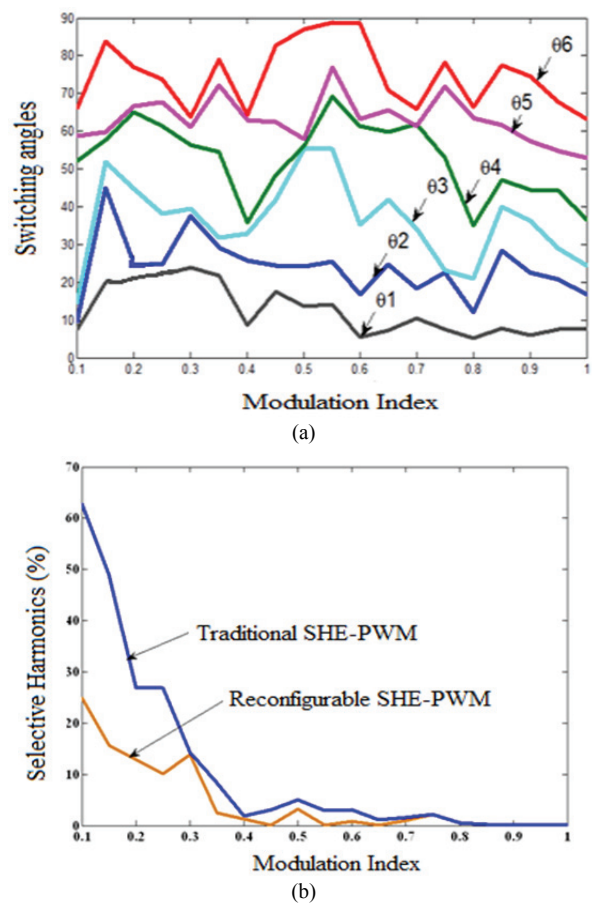

Fig. 5. Performance of the reconfigurable SHE-PWM technique: (a) Switching angles in the reconfigurable SHE-PWM; (b) Comparison of the traditional and reconfigurable SHE-PWM.

The current flows in series and remains the same in the entire H–bridge cell. Thus, the expression for power distribution in an individual H-bridge cell is expressed as a percentage of total power as shown in equation (15). The majority of the total power is handled by a high voltage cell.

$$Po_i = \frac{K_i So_i}{\sum_{i=1}^{n} K_i So_i} \tag{15}$$

VI. SIMULATION RESULTS

Fig. 5(a) shows switching angles obtained in the

TABLE VI
REDUNDANT SWITCHING STATES IN THE RECONFIGURABLE SHE-PWM

MI	Technique	θ_1^o	θ_2^o	θ_3^o	θ_4^o	θ_5^o	θ_6^o	
0.25	Traditional	HB 1 (Sa1,Sa2)	HB2 (Sb1,Sb2)	-	-	-	-	1
	Reconfigurable	HB1 (Sa1,Sa2)	0V	HB1 (Sa1,Sa2)	HB2 (Sb1,Sb2)	HB1 (Sa1,Sa2)	HB1 (Sa1,Sa2)	6
	Reconfigurable with Redundant	HB1 (Sa1,Sa2)	0V	HB2-HB1 (Sb1,Sb2) (Sa3,Sa4)	HB2 (Sb1,Sb2)	HB3-HB2 (Sc1,Sc2) (Sb3,Sb4)	HB3-HB2 (Sc1,Sc2) (Sb3,Sb4)	6
0.15	Traditional	HB1	-	-	-	-	-	-
	Reconfigurable	HB1 (Sa1,Sa2)	0V	HB1 (Sa1,Sa2)	0V	HB1 (Sa1,Sa2)	0V	6
	Reconfigurable with Redundant	HB1 (Sa1,Sa2)	0V	HB2-HB1 (Sb1,Sb2) (Sa3,Sa4)	0V	HB3-HB2 (Sc1,Sc2) (Sb3,Sb4)	0V	6

reconfigurable SHE-PWM technique considering the objective function shown in Table III. Fig. 5(b) reveals the fact that the percentage of the Selective Harmonics (SH) obtained in the reconfigurable SHE-PWM is drastically reduced in middle and low range of the MI when compared to the traditional SHE-PWM method. The optimized switching angles obtained in the BBO-MAS algorithm are tabulated in Table V and further employed for the simulation and experimental studies.

A. Switching frequency Reduction using Redundant States

The traditional SHE-PWM technique has a low switching frequency at an MI of 0.15 and is switched only once at θ1. However, only the fundamental component h1 is controlled, while the harmonics (h5, h7, h11, h13, h15) are more pronounced. In addition, the voltage is drawn only from the single DC source Vdc1. The remaining sources do not actively participate in the process.

In the reconfigurable SHE-PWM technique, the number of switching angles is maintained at six to eliminate all of the intended harmonics (h5, h7, h11, h13, h15). However, only a single combination of bridges (0, 0, HB1) is used. The switches (Sa1 and Sa2) in HB1 are switched on thrice at (θ_1, θ_3 and θ_5) and switched off at (θ_2, θ_4 and θ_6) in a quarter cycle. This results in higher number of switching angles when compared to the traditional SHE-PWM. Furthermore, the sources of HB2 and HB3 remain unutilized.

To have effective utilization for all of the H bridge cells and sources, and to share the switching numbers among the bridges, reconfigurable SHE-PWM with redundant states is explored. The redundant states for the generation of various voltage levels is shown in Fig. 6. To generate 1Vdc, three possible redundant states (R) exist with (HB3, HB2, HB1) as R1: (0, 0, HB1), R2: (0, HB2, -HB1) and R3: (HB3, -HB2, 0). The R1 combination is switched on at θ_1 and switched off at θ_2, the R2 combination is switched on at θ_3 and switched off at θ_4 and the R3 combination is switched on at θ_5 and switched off at θ_6. Similarly, to generate 2Vdc, three possible redundant state (R) exists with (HB3, HB2, HB1) as R1: (0, HB2, 0), R2: (HB3, 0, -HB1) and R3: (HB3, -HB2, HB1). From Table VI, it is inferred that even though the switching number increases, it is shared by a redundant combination among all of the H bridge cells and results in a reduction of the switching frequency of individual devices and effective utilization of all of the sources.

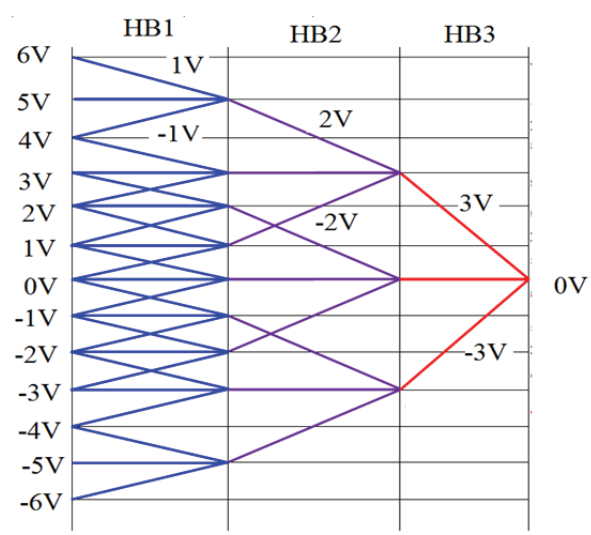

Fig. 6. Redundant switching states.

Simulations are performed in MATLAB/SIMULINK to validate the performance of the reconfigurable SHE-PWM technique. The output voltage and FFT spectrum in Fig. 7(a)-7(c) illustrates that in the reconfigurable SHE-PWM technique both the THD and the individual harmonic percentage are significantly reduced. It can be observed from Fig. 8(a)-8(c) that there is an enormous reduction in the individual harmonics (indicated by arrows) especially in the lower range of the MI 0.45, 0.25 and 0.15 while the DOF to control the harmonics remains at six.

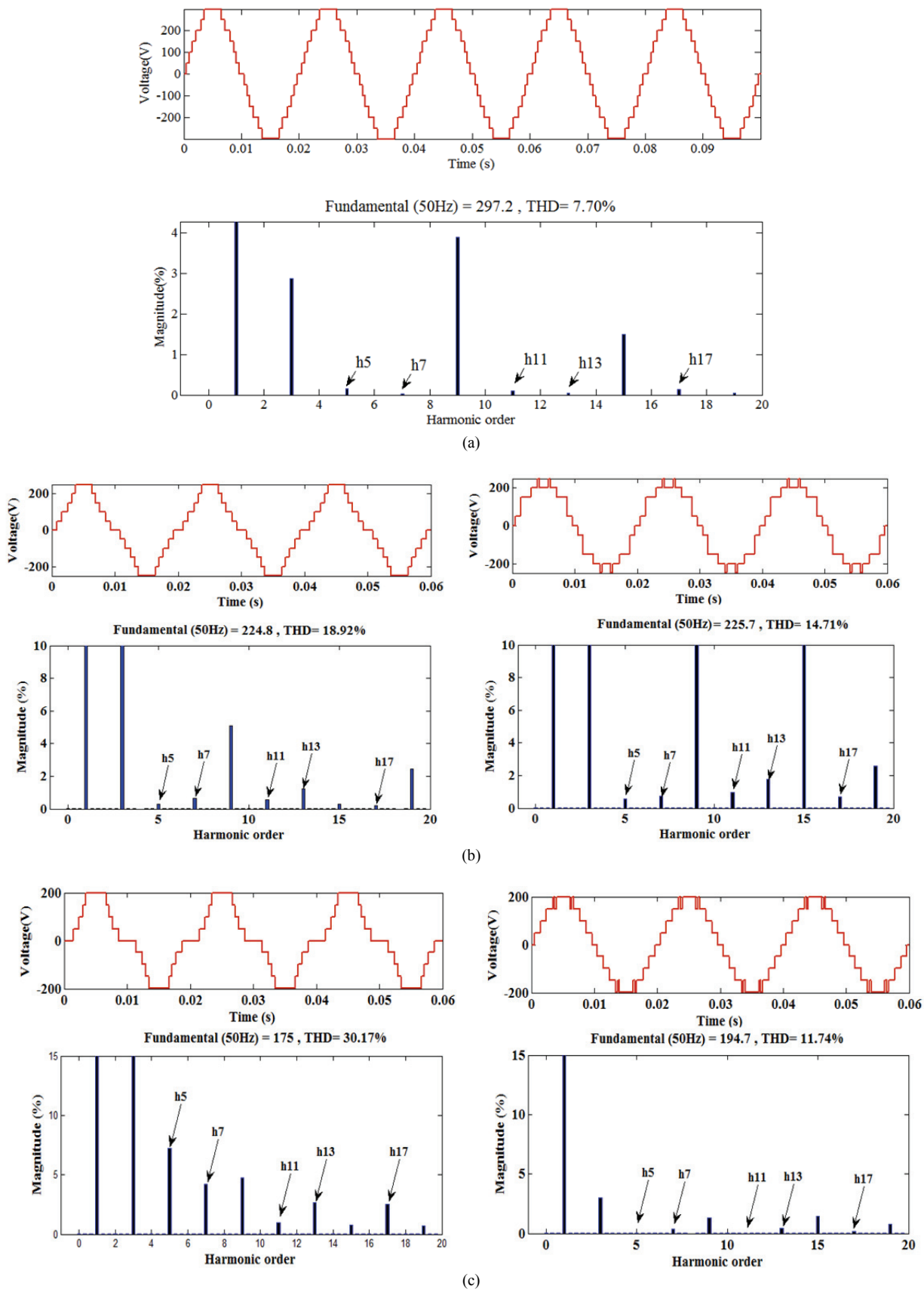

Fig. 7. Simulation results of the traditional and the reconfigurable SHE-PWM: (a) Traditional at MI =1; (b) Traditional and reconfigurable at MI=0.75; (c) Traditional and reconfigurable at MI=0.65.

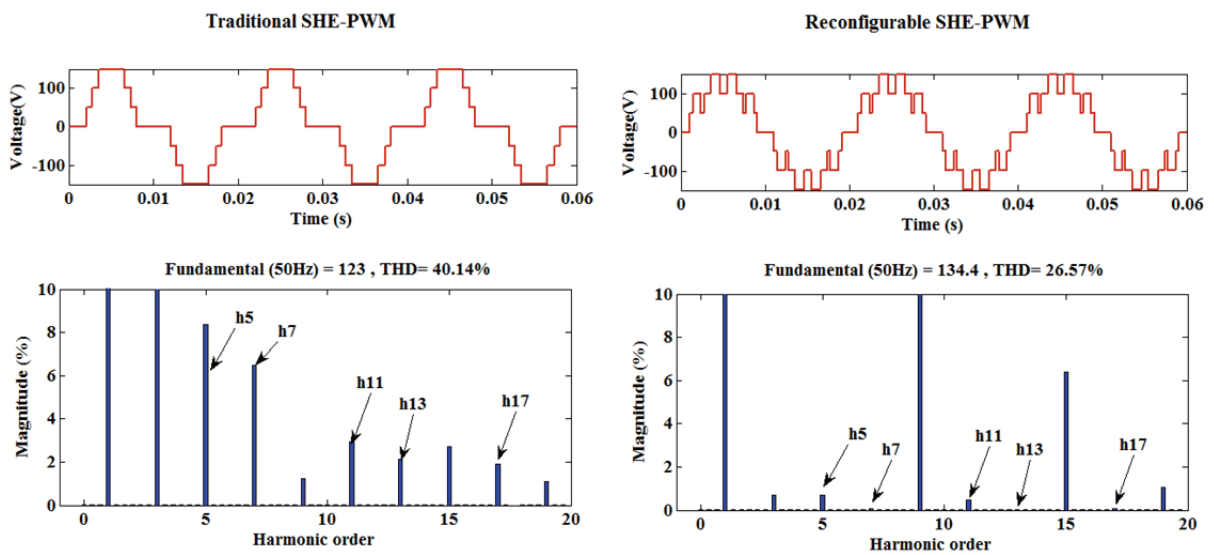

(a)

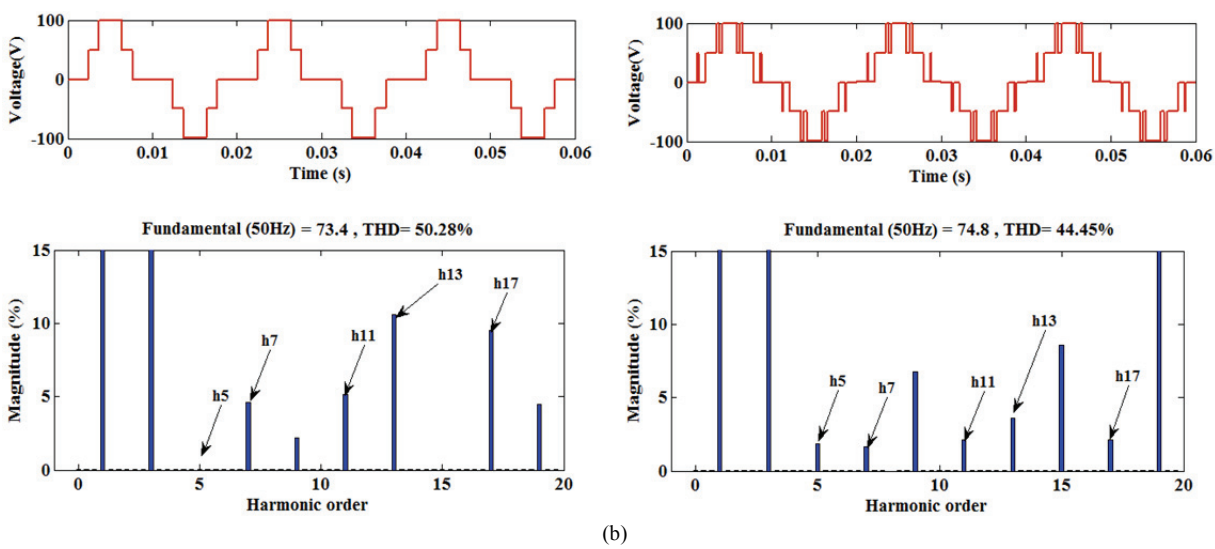

(b)

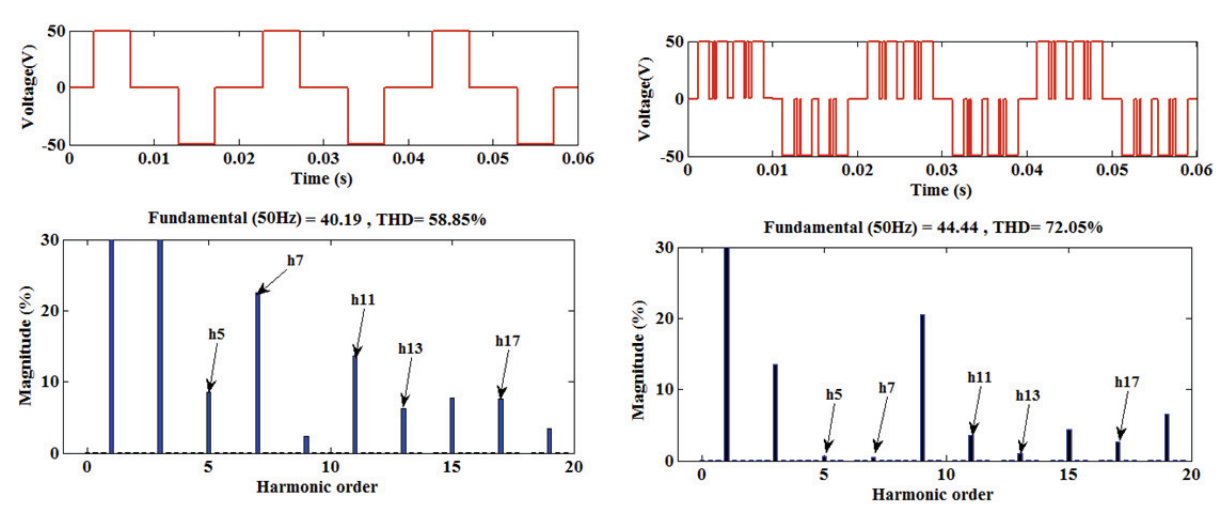

(c)

Fig. 8. Simulation results of the traditional and the reconfigurable SHE-PWM: (a) Traditional and reconfigurable at MI =0.45; (b) Traditional and reconfigurable at MI=0.25; (c) Traditional and reconfigurable at MI=0.15.

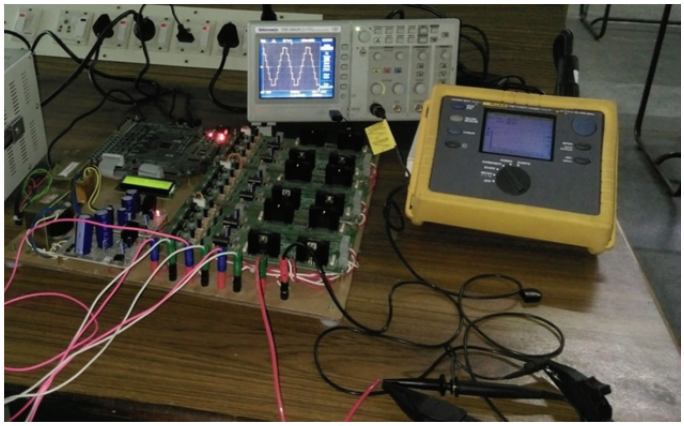

Fig. 9. Experimental set-up of an ACMLI.

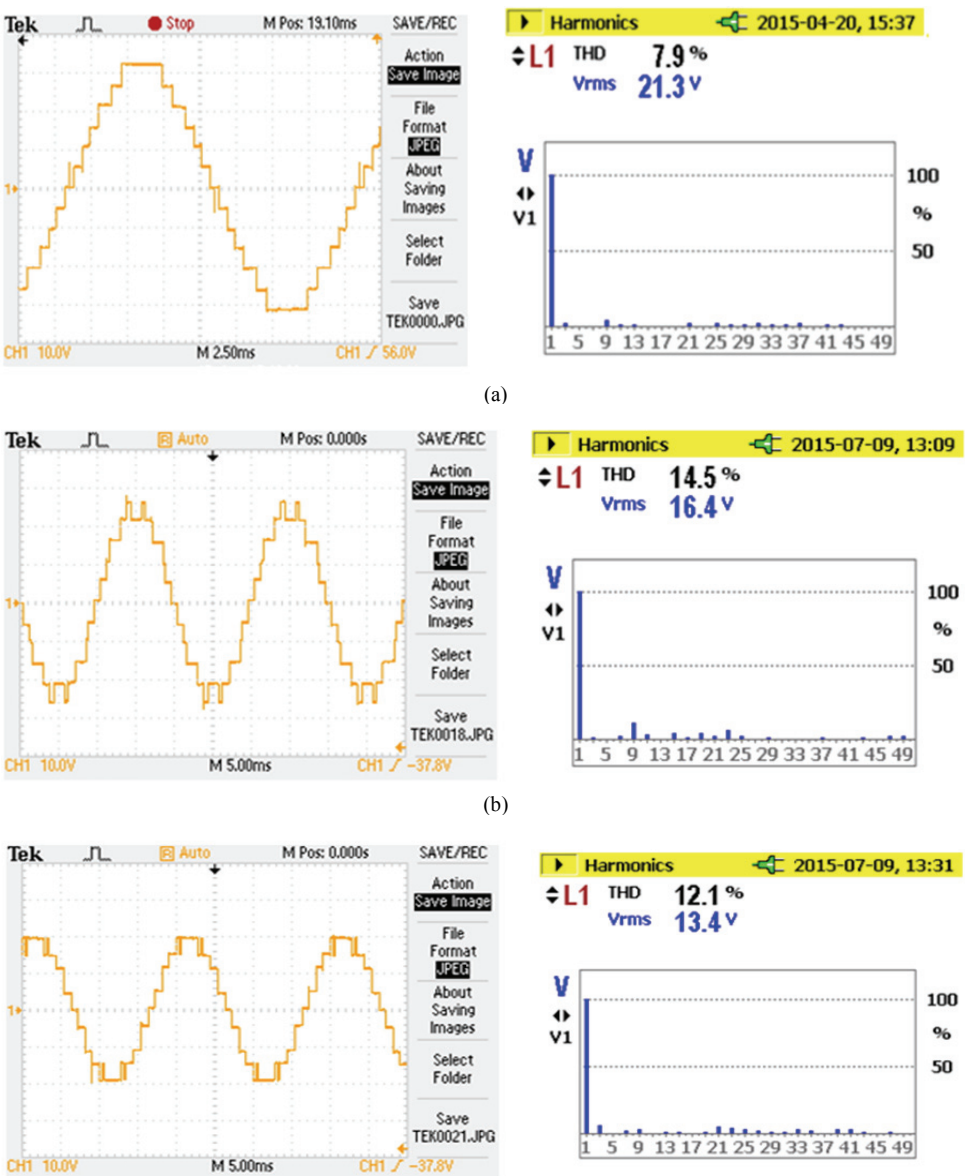

Fig. 10. Experimental voltage waveforms and corresponding FFT spectrum of the reconfigurable SHE-PWM technique: (a) MI=1; (b) MI=0.75; (c) MI=0.65.

TABLE VII
HARMONIC IN THE TRADITIONAL AND THE RECONFIGURABLE SHE-PWM

MI		DOF	h5 (%)	h7 (%)	h11 (%)	h13 (%)	h17 (%)
0.75	Traditional	5	0.2	0.6	0.5	1.3	0.2
	Reconfigurable	6	0.2	0.6	0.9	0.3	0.2
0.65	Traditional	4	7.1	4.5	1	3.2	3
	Reconfigurable	6	0	0.3	0	0.33	0
0.45	Traditional	3	8.3	6.8	3.7	2.8	2.3
	Reconfigurable	6	0.8	0	0.3	0	0
0.25	Traditional	2	0	4.7	5.6	10.6	9
	Reconfigurable	6	2.6	2.5	2.8	3.8	2.6
0.15	Traditional	1	8	22	15	6	6.2
	Reconfigurable	6	0.1	0.1	4	1	2.8

TABLE VIII
EXPERIMENTAL SPECIFICATION

Parameters	Values
Number of H bridge cells	3
FPGA	DS312 Spartan 3E
MOSFET	IRF340
R Load	30Ω
L Load	30mH
FFT analyzer	Fluke 1735 power logger

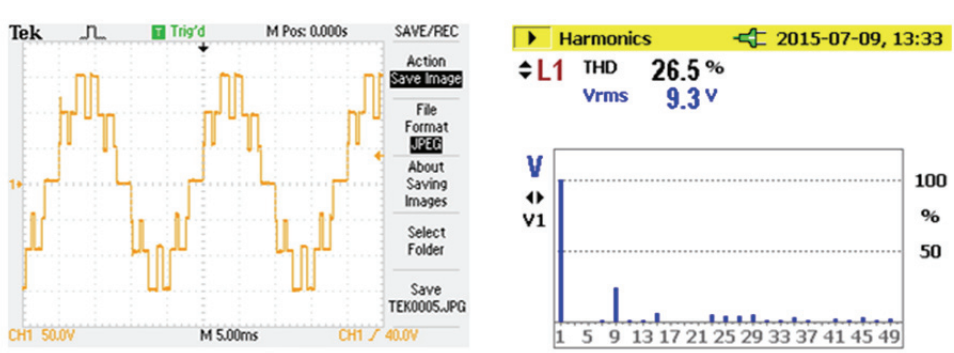

(a)

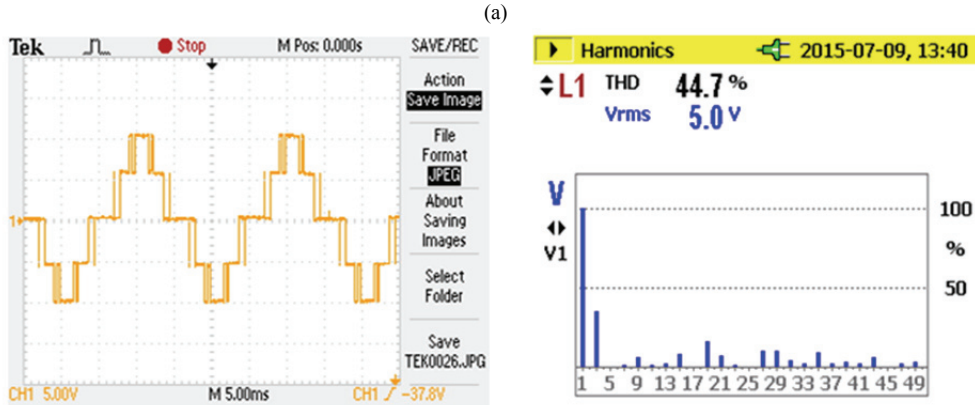

(b)

Fig. 11. Experimental voltage waveforms and corresponding FFT spectrum of the reconfigurable SHE-PWM technique: (a) MI=0.45; (b) MI=0.25.

TABLE IX
COMPARISON OF THE RECONFIGURABLE SHE-PWM IN THIRTEEN-LEVEL ACMLI

References	Algorithm	Level	Number of cells	Range of MI
[19]	PSO	7	3	0.4-0.85
[20]	MCSA -SAM	9	4	0.4 -1
[22]	Reference synthesize	12	6	1
[16]	PSO-NR	11	5	0.6 -1
[17]	ANFIS/ABC	7	3	0.5 -1
[18]	DE	9	4	0.5–0.93
[26]	GA	13	3	1
Proposed	BBO-MAS	13	3	0.25 -1

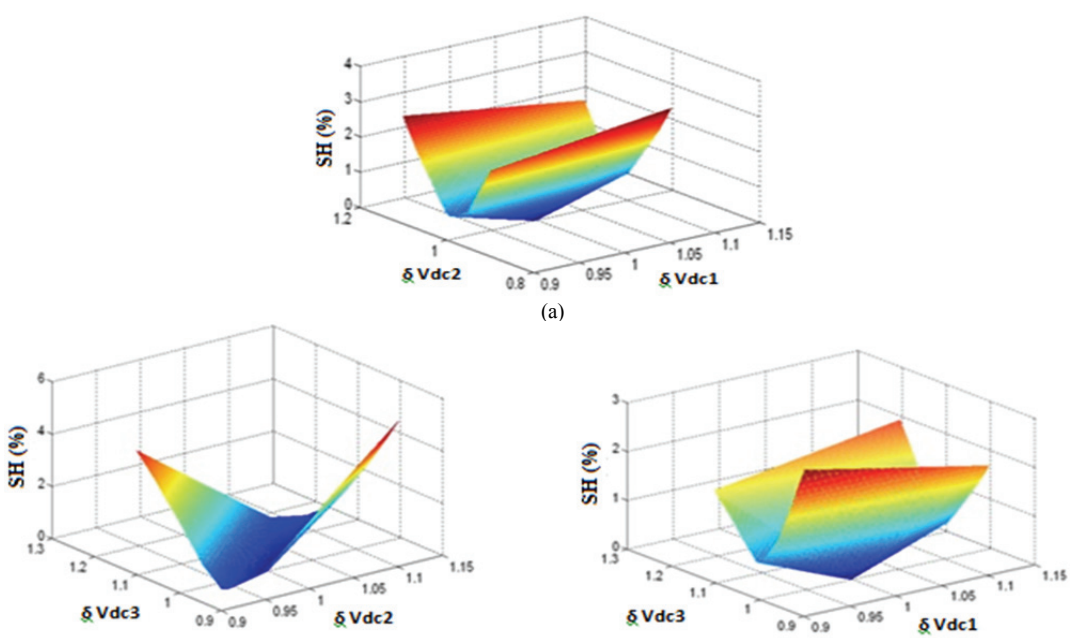

(a)

(b) (c)

Fig. 12. Selective harmonics with variations in the non-integer dc source voltages: (a) Variations in Vdc1 and Vdc2; (b) Variations in Vdc2 and Vdc3; (c) Variation in Vdc1 and Vdc3.

The targeted harmonics (h5, h7, h11, h13, h15) obtained in the simulation are tabulated in Table VII. The individual targeted harmonic components are reduced to below 1% in the range of MI ≥ 0.25 and to below 3% in the MI range of 0.25 -1. It is also observed that at a very low MI of 0.15 in the traditional SHE-PWM the individual harmonic value remains at 22%. Meanwhile, with the reconfigurable SHE-PWM, the performance is enhanced with a very low harmonic distortion of less than 3%. The reconfigurable SHE-PWM satisfied the standards of IEEE 519, in which the individual harmonic components in power systems are limited to less than 3%.

VII. EXPERIMENTAL RESULTS

The proposed reconfigurable SHE-PWM is implemented as a hardware prototype as shown in Fig. 9. The specifications of the prototype are represented in Table VIII. The switching angle is loaded into the FPGA and the switching signal is isolated from the power circuit by an opto-coupler 6N137. The results are demonstrated with the proposed reconfigurable SHE-PWM technique for a thirteen-level ACMLI. Selected operating points in correspondence with the simulation results are utilized for the hardware verification.

Fig. 10(a)-(c) depicts experimental voltage waveforms and FFT spectrum measured using a fluke power logger for the higher range of MI, while Fig. 11 (a)-(b) is obtained for lower range of MI. The FFT spectrum obtained by the fluke power analyzer has validated the elimination of all the targeted harmonics (h5, h7, h11, h13, h17). The experimental results with the reconfigurable SHE-PWM technique are in agreement with the simulation results with the elimination of all the targeted harmonics. The proposed reconfigurable SHE-PWM technique is compared with methods in the

literature and it has been shown to give an extended operating range of the MI from 0.25 to 1 when compared to the other methods as shown in Table IX.

A. Non-Integer DC Sources

The SH(%) and THD are analyzed in simulations with variations in the dc sources (δVdc) under the SHE-PWM technique. The variations are plotted in a 3-dimensional view in MATLAB. The SH(%) is increased to a maximum of: 2.48% for variations in Vdc1 and Vdc2. as shown in Fig. 12(a); 4.53% with variation in Vdc2 and Vdc3, as shown in Fig. 12(b); and 1.5% for variation in Vdc1 and Vdc3, as shown in Fig. 12(c). It is observed that the SH(%) is at its minimum (almost completely eliminated) only at an integer ratio of 1:2:3.

VIII. Conclusions

The proposed reconfigurable SHE-PWM technique has enhanced the harmonic spectrum over a wide range of MI in a thirteen-level ACMLI. In reconfigurable SHE-PWM the MI region is segmented into six sectors. In addition, different switching patterns and different distributions of the switching angles are derived for each sector. A memetic BBO-MAS hybrid algorithm is applied to solve the reconfigurable SHE-PWM technique and the optimal solutions of the switching angles are obtained. The effectiveness of the proposed reconfigurable SHE-PWM technique is tested under various operating points of MI, and the FFT spectrum is validated by simulation and experimental results. The targeted harmonics are eliminated to a significant extent over a wide range of MI in the reconfigurable SHE-PWM technique when compared to the traditional SHE-PWM technique.

References

[1] J. Rodriguez, J. S. Lai, and Z. P. Fang, "Multilevel inverters: A survey of topologies, controls and applications," *IEEE Trans. Ind. Electron.*, Vol. 49, No. 4, pp. 724-738, Aug. 2002.

[2] L. G. Franquelo, J. Rodriguez, J. I. Leon, S. Kouro, and R. Portillo, "The Age of multilevel converters arrives," *IEEE Ind. Electron. Mag* , Vol. 2, No. 2, pp. 28-39, Jun. 2008.

[3] A. Mahrous and E. Hendawi, "A new single-phase asymmetrical cascaded multilevel DC-link inverter," *J. Power Electron.,* Vol. 1 No.4, pp 1504-1512, Jul. 2016.

[4] B. Ozpineci, L. M. Tolbert, and J. N. Chiasson, "Harmonic optimization of multilevel converters using genetic algorithms," *IEEE Power Electron. Lett.*, Vol. 3, No. 3, pp. 92-95, Sep. 2005.

[5] A. Moeini, H. Iman-Eini, and M. Najjar, "Non-equal DC link voltages in a cascaded H-bridge with a selectiveharmonic mitigation-PWM technique based on the fundamental switching frequency," *J. Power Electron.*, Vol. 17, No. 1, pp. 106-114, Jan. 2017.

[6] M. R. Banaei and P. A. Shayan, "Solution for selective harmonic optimization in diode-clamped inverters using radial basis function neural networks," *IET Power Electron.*, Vol. 7, No. 7, pp. 1797-1804, Mar. 2014.

[7] Y. S. Kumar and G. Poddar, "Control of medium-voltage AC motor drive for wide speed range using modular multilevel converter," *IEEE Trans. Ind. Electron.*, Vol. 64, No. 4, pp. 2742-2749, Apr. 2017.

[8] J. Cao, H. Liu, P. Ding, B. Yang, and S. Xie, "Wide correction range three-level dynamic voltage corrector," *IEEE Trans. Power Electron.,* Vol. 31, No. 9, pp. 6217-6225, Sep. 2016.

[9] J. N. Chiasson, L. M. Tolbert, K. J. McKenzie, and Z. Du, "Elimination of harmonics in a multilevel converter using the theory of symmetric polynomials and resultants," *IEEE Trans. Contr. Syst. Technol.*, Vol. 13, No. 2, pp. 216-223, Mar. 2005.

[10] K. Yang, Q. Zhang, R. Yuan, W. Yu, and J. Wang, "Selective harmonic elimination with Groebner bases and symmetric polynomials," *IEEE Trans. Power Electron.,* Vol. 31, No. 4, pp. 689-694, Apr. 2015.

[11] R. N. Ray, D. Chatterjee, and S. K. Goswami, "An application of PSO technique for harmonic elimination in a PWM inverter," *Applied Soft Computing*, Vol. 9, No. 4, pp. 1315-1320, Sep. 2009.

[12] V. Roberge, M. Tarbouchi, and F. Okou, "Strategies to accelerate harmonic minimization in multilevel inverters using a parallel genetic algorithm on graphical processing unit," *IEEE Trans. Power Electron.*, Vol. 29, No. 10, pp. 5087-5090, Oct. 2014.

[13] M. T. Hagh, H. Taghizadeh and K. Razi, "Harmonic minimization in multilevel inverters using modified species-based particle swarm optimization," *IEEE Trans. Power Electron.*, Vol. 24, No. 10, pp. 2259-2267, Oct. 2009.

[14] Z. Salam, A. M. Amjad, and A. Majed, "Design and implementation of 15-level cascaded multi-level voltage source inverter with harmonics elimination pulse-width modulation using differential evolution method," *IET Power Electron.*, Vol. 8, No. 9, pp. 1740-1748, Jun. 2015.

[15] M. S. A. Dahidah, G. Konstantinou, and V. G. Agelidis, "A review of multilevel selective harmonic elimination PWM: Formulations, solving algorithms, implementation and applications," *IEEE Trans. Power Electron.*, Vol. 30, No. 8, pp. 4091-4106, Aug. 2015.

[16] K. Shen, D. Zhao, J. Mei, L. M. Tolbert, J. Wang, M. Ban, Y. Ji, and X. Cai. "Elimination of harmonics in a modular multilevel converter using particle swarm optimization-based staircase modulation strategy," *IEEE Trans. Ind. Electron.*, Vol. 61, No. 10, pp. 5311-5322, Oct. 2014.

[17] H. R. Baghaee, M. Mirsalim, G. B. Gharehpetian, H. A. Talebi, and A. Niknam-Kumle, "A hybrid ANFIS/ ABC-based online selective harmonic elimination switching pattern for cascaded multi-level inverters of microgrids," *IEEE Trans. Ind. Electron.,* to be published.

[18] A. M. Amjad, Z. Salam, and A. M. A. Saif, "Application of differential evolution for cascaded multilevel VSI with harmonics elimination PWM switching," *International Journal of Electrical Power and Energy Systems*, Vol. 64, pp. 447-456, Jan. 2015.

[19] V. G. Agelidis, A. I. Balouktsis, and M. S. Dahidah, "A five-level symmetrically defined selective harmonic elimination PWM strategy: Analysis and experimental validation," *IEEE Trans. Power Electron.*, Vol. 23, No. 1, pp. 19-26, Jan. 2008.

[20] H. R. Massrur, T. Niknam, and M. Mardaneh, "Harmonic elimination in multilevel inverters under unbalanced voltages and switching deviation using a new stochastic strategy," *IEEE Trans. Ind. Informat*., Vol. 12, No. 2, pp.716-725, Apr. 2016.

[21] M. H. Etesami, N. Farokhnia, and S. Hamid Fathi, "Colonial competitive algorithm development toward harmonic minimization in multilevel inverters," *IEEE Trans. Ind. Informat*., Vol. 11, No. 2, pp. 459-466, Apr. 2015.

[22] P. L. Kamani and M. A Mulla, "Middle-level SHE pulse-amplitude modulation for cascaded multilevel inverters," *IEEE Trans. Ind. Electron.*, Vol. 65, No. 3, pp. 2828-2833, Mar. 2018.

[23] M. Etesami, N. Ghasemi, D. M. Vilathgamuwa, and W. L. Malan, "Particle swarm optimisation-based modified SHE method for cascaded H-bridge multilevel inverters," *IET Power Electron.*, Vol. 10, No. 1, pp. 18-28, Jan. 2017.

[24] A. Moeini, H. Iman-Eini, and A. Marzoughi, "DC link voltage balancing approach for cascaded H-bridge active rectifier based on selective harmonic elimination-pulse width modulation," *IET Power Electron.*, Vol. 8, No. 4, pp. 583-590, Feb. 2015.

[25] N. Farokhnia, S. H. Fathi, R. Salehi, G. B. Gharehpetian, and M. Ehsani, "Improved selective harmonic elimination PWM Strategy in multilevel inverters," *IET Power Electron.*, Vol. 5, No. 9, pp. 1904-1911, Nov. 2012.

[26] W. A. Halim, N. A. Rahim, and M. Azri, "Selective Harmonic Elimination for a single phase 13-level TCHB based cascaded multilevel inverter using FPGA," *J. Power Electron.*, Vol. 14, No. 3, pp. 488-498, May. 2014.

[27] D. Simon, "Biogeography-based optimization," *IEEE Trans. Evol. Comput*., Vol. 12, No. 6, pp. 702-713, Dec. 2008.

[28] Y. Ahn, J. Park, C. G. Lee, J. Kim, and S. Jung, "Novel memetic algorithm implemented with GA and MADS for optimal design of electromagnetic system," *IEEE Trans. of Magn.*, Vol. 46, No. 6, pp. 1982-1985, Jun. 2010.

[29] A. K. Bansal, R. Kumar, and R. A. Gupta, "Economic analysis and power managment of a small autonomous hybrid power system (SAHPS) using biogeography based optimization (BBO) algorithm," *IEEE Trans. Smart Grid*, Vol. 4, No. 1, pp. 638-648, Mar. 2013.

[30] S. H. Yang and J. F. Kiang, "Optimization of asymmetrical difference pattern with memetic algorithm," *IEEE Trans. Antennas Propag.*, Vol. 62, No. 4, pp. 2297-2302, Apr. 2014.

[31] Y. Ahn, J. Park, C. G. Lee, J. Kim, and S. Y. Jung, "Novel memetic algorithm implemented with GA and MADS for optimal design of electromagnetic system," *IEEE Trans. of Magn.*, Vol. 46, No. 6, pp. 1982-1985, Jun. 2010.

Kavitha R received her B.E. degree in Electronics and Communication Engineering from Bharathiar University, Coimbatore, India, in 2001; her M.E degree in Power Electronics and Drives from College of Engineering, Guindy, Anna University, Chennai, India, in 2004; and her Ph.D. degree from Anna University, Chennai, India, in 2015. She has one decade of teaching experience in undergraduate and post graduate courses of Electrical and Electronics engineering. She is presently working as an Associate Professor in the Department of Electrical and Electronics Engineering, Kumaraguru College of Technology, Coimbatore, India. Her current research interests include power electronics, multilevel inverters, integration of renewable energy sources, optimization techniques and active harmonic analysis.

Rani Thottungal received her B.E. degree in Electrical and Electronics Engineering and her M.E degree in Power System from Andhra University, Visakhapatnam, India, in 1989 and 1993, respectively. She received her Ph.D. degree from Bharathiar University, Coimbatore, India, in 2008. She has two decade of teaching experience in Electrical and Electronics engineering. She is presently working as a Professor in the Department of Electrical and Electronics Engineering, Kumaraguru College of Technology, Coimbatore, India. Her current research interests include restructured power systems, circuits and control, and the integration of renewable energy sources.